HHS Public Access

Author manuscript

Drug Dev Ind Pharm. Author manuscript; available in PMC 2017 November 01.

Published in final edited form as:

Drug Dev Ind Pharm. 2016 November ; 42(11): 1833–1841. doi:10.1080/03639045.2016.1178769.

Optimization of hot melt extrusion parameters for sphericity and hardness of polymeric face-cut pellets

Abdullah S. Alshetaili[1,2], **Bjad K. Almutairy**[1], **Saad M. Alshahrani**[2], **Eman A. Ashour**[1], **Roshan V. Tiwari**[1], **Sultan M. Alshehri**[3], **Xin Feng**[1], **Bader B. Alsulays**[2], **Soumyajit Majumdar**[1], **Nigel Langley**[4], **Karl Kolter**[5], **Andreas Gryczke**[6], **Scott T. Martin**[7], and **Michael A. Repka**[1,8,*]

[1]Department of Pharmaceutics and Drug Delivery, School of Pharmacy, The University of Mississippi, University, MS 38677, USA

[2]Department of Pharmaceutics, College of Pharmacy, Prince Sattam Bin Abdulaziz University, Alkharj, Saudi Arabia

[3]Department of Pharmaceutics, College of Pharmacy, King Saud University, Riyadh, Saudi Arabia

[4]BASF Corporation, 500 White Plains Road, Tarrytown, NY, 10591, USA

[5]BASF SE, R&D Project, Management Excipients, Ludwigshafen, 67056, Germany

[6]BASF SE, Global Development and Technical Marketing, Ludwigshafen, 67056, Germany

[7]Thermo Fisher Scientific, Tewksbury, MA, 01876, USA

[8]Pii Center for Pharmaceutical Technology, The University of Mississippi, University, MS 38677, USA

Abstract

The aim of this study was to formulate face-cut, melt extruded pellets and to optimize hot melt process parameters to obtain maximized sphericity and hardness by utilizing Soluplus® as a polymeric carrier and carbamazepine (CBZ) as a model drug. Thermal gravimetric analysis (TGA) was used to detect thermal stability of CBZ. The Box-Behnken design for response surface methodology was developed using three factors, processing temperature (°C), feeding rate (%), and screw speed (rpm), which resulted in 17 experimental runs. The influence of these factors on pellet sphericity and mechanical characteristics was assessed and evaluated for each experimental run. Pellets with optimal sphericity and mechanical properties were chosen for further characterization. This included differential scanning calorimetry, drug release, hardness friability index (HFI), flowability, bulk density, tapped density, Carr's index, and fourier transform infrared radiation (FTIR) spectroscopy. TGA data showed no drug degradation upon heating to 190°C. Hot melt extrusion (HME) processing conditions were found to have a significant effect on the pellet shape and hardness profile. Pellets with maximum sphericity and hardness exhibited no crystalline

[*]**Address for correspondence:** Michael A. Repka, D.D.S.,Ph.D., Professor and Chair, Department of Pharmaceutics and Drug Delivery, Director, Pii Center for Pharmaceutical Technology, School of Pharmacy, The University of Mississippi, University, MS 38677, Phone: 662-915-1155, Fax: 662-915-1177, marepka@olemiss.edu.

Declaration of interest: The authors have no conflicts of interest to disclose.

peak after extrusion. The rate of drug release was affected mainly by pellet size, where smaller pellets released the drug faster. All optimized formulations were found to be of superior hardness and not friable. The flow properties of optimized pellets were excellent with high bulk and tapped density.

Keywords

Sphericity; Hardness; Hot-melt extrusion; Face-Cut Pellets; Design of experiment; Box-Behnken design; Soluplus®; carbamazepine

INTRODUCTION

Hot-melt extrusion (HME) is a continuous manufacturing process in which an extrudate is obtained by forcing the active drug and excipients through the die under controlled conditions, including temperature, mixing, feed-rate, and pressure[1]. This process is used to achieve solid dispersions or solid solutions, which may have the potential to increase solubility, dissolution rate, and the bioavailability of poorly water soluble active pharmaceutical ingredients (APIs)[2–4]. HME overcomes some of the limitations of traditional manufacturing techniques such as spray drying or freeze drying, including solvent usage and multiple processing steps[5]. However, during the formulation of HME products, there are several obstacles that need to be overcome. First, the influence of the variable HME process parameters on the processing material must be optimized based on the final goal[6, 7]. Second, identification of the combination among API, carrier, and additives is necessary for achievement of the desired final dosage form[8]. Third, the downstream processing needs to be optimized based on the intended final dosage form[9]. Commonly, extrudates are milled and used to fill capsules[10], compressed into tablets[11], or shaped using a downstream-adapted pelletizer[12]. In this study, the strand of a certain material composition is shaped into spherical pellets using a face-cut pelletizer to avoid the downstream processing and overcome the above limitation.

Face–cut pelletizing is an innovative technology where the hot, molten strand is cut directly into small pellets by a rotating knife immediately after exiting the die. The cutting takes place above the softening point, and the pellets are transported to the cyclone by a vacuum where viscous forces, like surface tension, act as a driving force that allows the pellets to contract and become spherical[9, 13]. Extrusion–spheronization is the typical way of producing spherical pellets[14–16]. After extrusion, the extrudate is cut or broken into cylindrical pieces and spheronized in an extra, discontinuous step. During spheronization, irregularly shaped material is heated, with or without a heated spheronizer, to a softening temperature to make rounded pellets. Further spheronizing steps are unnecessary when using face-cut pelletization. Combining HME with face-cut pelletization offers an outstanding advantage, because spherical pellets can be produced using a single continuous step.

Numerous studies have reported the production of nearly spherical pellets by face-cut pelletization and evaluated the influence of formulation composition and process parameters on the morphology of pellets. Roblegg et al. (2011) reported the use of calcium stearate (CaSt) as a thermoplastic excipient for preparation of face-cut pellets, which are cooled

externally[17]. Bialleck and Rein (2011) have reported the development of starch-based face-cut pellets containing different APIs[18]. The two studies have found that the morphology of pellets depends on the composition of formulations and process parameters. In this study, we used a novel air-cooled face-cut pelletizer connected to a pipe (tube), where the air pushed pellets through it into the cyclone. The synergistic effect of viscous forces, like surface tension, with high rotation speed in the cyclone resulted in superior spherical shape.

In order for pellets to be accepted as a dosage form and administered to patients, they should have certain physico-mechanical characteristics, such as sphericity, good flow property, ease of dosing, compact structure, and smooth surface with high bulk density[19]. Sphericity is one of the important measurements for assessing quality of pellets. Highly spherical pellets flow easily, which is considered ideal for automated processes (tableting, capsule filling, and packaging), where maintaining exact dosing is required[20]. It is also necessary for pellets to possess sufficient mechanical strength to withstand the mechanical forces associated with the manufacturing process[21]. The aim of this study was to formulate face-cut, melt extruded pellets and to optimize hot melt process parameters on pellets to obtain maximized sphericity and hardness utilizing Soluplus® as a polymeric carrier and carbamazepine (CBZ) as a model drug.

MATERIALS AND METHODS

Materials

CBZ was purchased from Afine Chemicals Limited (Zhejiang, China). Polyvinyl caprolactam–polyvinyl acetate–polyethylene glycol graft copolymer (PVCL–PVAc–PEG, Soluplus®) were kindly donated by BASF SE (Ludwigshafen, Germany). All other chemicals used were of analytical grade and obtained from either Fisher Scientific (Waltham, MA, USA) or Spectrum Chemicals (New Brunswick, NJ, USA).

Methods

Thermal gravimetric analysis—The thermal stability of the physical mixture and CBZ was detected at the employed extrusion temperatures using a Perkin Elmer Pyris 1 thermogravimetric analyzer (TGA) (Waltham, MA, USA). The Pyris manager software (Perkin Elmer Life and Analytical Sciences) was used for running the instrument and analyzing the data. Three to 4 mg of physical mixture was weighed and heated from 20°C to 250°C at 10°C/min under a controlled atmosphere of nitrogen. Percent weight loss was plotted against temperature to determine weight loss.

Hot melt process—The polymer was screened using a USP #35 mesh screen. The subjected polymer was pre-plasticized with propylene glycol (3%) to prevent sudden stop of the extruder due to high torque at low temperature with high screw speed. CBZ, which has a high melting point (193°C), was blended with Soluplus® (the glass transition temperature is 70°C) at 10% drug loading using a V-shell blender. The blend was extruded using a co-rotating twin-screw hot melt extruder connected to an air-cooled face-cut pelletizer. HME was performed at different levels of processing temperatures, feeding rates, and screw speeds to optimize the ranges that yielded pellets. The die plate was coupled with a nozzle

and attached to the face-cut pelletizer by screws. Face-cut pelletizer had a blower unit that generated air that pushed the pellets cut at the die plate into the cyclone through a pipe. The face cutter speed was kept constant at 70 rpm. Pellets started rotating at the cyclone under high speed with high amount of air and fall down into a basket.

Design of experiment—The Box-Behnken design for response surface methodology was developed using Design Expert® 8.0.6 (Stat-Ease, Inc., Minneapolis, MN, USA). The optimized ranges and level of the variables are shown in Table 1.

This design requires an experimental number of runs calculated as follows:

$$N=k^2+k+cp \quad (1)$$

Where, k is the factor number, 3 in this case, and cp is the number of replications at the center point, 5 in this case. The design resulted in 17 experimental runs, as shown in Table 2. The three dimensions of the cube correspond to three factors, processing temperature (°C), feeding rate (%), and screw speed (rpm). The center point is a white circle to illustrate that this particular set of levels was replicated five times in this design, allowing for strong estimation of variance (Fig. 1).

Differential scanning calorimetry—Differential scanning calorimetry was utilized to analyze the samples. Three to 5 mg of milled pellets was analyzed at 10 °C/min heating rate between 30°C and 200 °C. Pyris™ manager software was used to calculate peak temperature at melting.

High-performance liquid chromatography (HPLC) method—The drug content was determined by a Waters HPLC consisting of Waters 600 binary pump, Waters 2489 UV detector, and Waters 717 plus auto sampler (Waters Technologies Corporation, Miliford, MA, USA). The stationary phase of the column was a Waters Symmetry shield C18, 250 × 4.6 mm, 5 μm particle size, reverse phase. The mobile phase was methanol, water, and acetic acid (34:65:1 % *v/v*) at a flow rate of 1 ml/min, and the ultraviolet (UV) detector was set at 285 nm wavelength[22]. Drug content of pellets was analyzed by dissolving the pellets in mobile phase and pre-filtering through a 0.45-μm filter and injected at volume of 20 μl. samples obtained from dissolution studies were collected precisely at pre-determined intervals and replaced with equal amounts of fresh dissolution medium, filtered and injected (Type II dissolution apparatus at a paddle speed of 100 rpm containing 900 ml of water). All studies were performed as replicates of five. The drug release profiles were compared by using the similarity factor (f2 value).

Determination of sphericity and pellets size—In order to determine the sphericity of the pellet, the shape and the area of pellets were investigated by optical microscopic image analysis[23]. Thirty pellets were selected randomly, and images were taken by Nikon Eclipse E600 Pol microscope equipped with a Nikon DS-Fi 1 camera (Tokyo, Japan). The images were taken under a top source of light on a black background to reduce the shadow. Image

analysis software was used to calculate area and perimeter. Circulatory factor (S) was calculated using the equation[24]:

$$S=12.56\,(A)\,/p^2 \quad (2)$$

Where, A is the area (cm^2) and p is the perimeter (cm).

Aspect ratio (AR) of optimized formulations was calculated from the following equation[25]:

$$(AR)=d_{max}/d_{min} \quad (3)$$

Where, d_{max} and d_{min} are the maximum and minimum Feret diameters measured by the software, respectively.

The microscope was fitted with ocular and stage micrometers, and the size of the optimized formulation was calculated as an average of 30 pellets.

Determination of hardness—Pellet Hardness was measured using a Tablet Hardness Tester (Model VK 200, Vankel Industries, Cary, NC, USA). Thirty pellets were selected randomly, and each pellet was placed in the center against the face plate of the sensing jaw. The force applied was continuously measured and recorded until the initial fracture of the pellet was detected and confirmed.

Physical characterization data of optimized pellets

Hardness friability index (HFI): HFI was measured using Electrolab Friability testing apparatus (Vankel Vanderkamp Friabilator). Thirty gm of the optimized pellets were uniformly tumbled for 20 min at 25 rpm. The tested pellets were gently tapped on ASTM # 35 mesh and were carefully collected, and the loss in weight was measured. HFI (%) was calculated using Equation 4:

$$HFI\ (\%)=(Fa/Fb)\times 100 \quad (4)$$

Where, Fb and Fa are the weights of the pellet before and after friability test.

Flowability: To determine the flow property of the pellets, flow rate was evaluate by using Flowdex® (Hanson Research Corporation, Chatsworth, CA, USA). The flowability apparatus was equipped with 10 mm orifice. Thirty gram of the pellets were weighed and filled into a funnel fixed on a clamp. The time was recorded from starting the pellets flow through orifice until finish in a beaker placed on electronic balance. The flow rate was expressed as $g.s^{-1}$.

Bulk density, tapped density, and Carr's index: The bulk density was calculated as the ratio of weight to the occupied volume. The optimized pellets were poured into a previously weighed graduated glass cylinder, and the weight to occupy the volume was determined.

Bulk density was calculated as M/Vi, where M is weighed mass and Vi is the initial unsettled apparent volume (n=5). Tapped density was calculated as M/Vf, where M is weighed mass and Vf is the final tapped volume (n=5). Carr's (Compressibility) index was measured according to following equation[26]:

$$\text{Carr's Index} = (\text{tapped density} - \text{bulk density}) \times 100 / \text{tapped density} \quad (5)$$

RESULTS AND DISCUSSION

Thermogravimetric analysis

The thermal stability of drug and physical mixture at employed extrusion temperatures were evaluated. The data showed no drug degradation when heated to 190°C (data not shown). Formulations were processed below this temperature to maintain the thermal stability of the drug.

Screening HME ranges

HME was performed to optimize the maximum and minimum ranges of processing parameters that yielded pellets with acceptable mean size. The minimum screw speed to maintain a continuous process was found to be 100 rpm. The extrusion temperature greatly influences the rheological properties of a molten formulation, which dictates the pelletization characteristics of the formulation tested. The temperature range was found to between from 120 and 150°C. The extruder barrels stopped below 120°C due to high torque, and the extrudate became more molten above 150°C, leading to loss of pelletization characteristics. The feed rate affected the size of the pellets, the screw speed, and extrusion temperatures. A feeding rate of 7% was found to be the maximum feeding rate that resulted in a mean pellet size at around 2 mm.

Design of experiment

The influence of extrusion temperature, feeding rate, and screw speed were evaluated in a quantitative way using response surface curves. The proposed second-degree polynomial was fitted to the data presented in Table 2 using multiple linear regressions to determine the optimum HME conditions that resulted in maximum sphericity and hardness. The predicted levels of sphericity (R1) and hardness (R2) are given in Table 2 and were calculated using Equation (6) and (7), respectively.

$$\begin{aligned} R1 = {} & 0.871 + 0.117 * A + 0.0355 * B \\ & - 0.0015 * C \\ & - 0.01975 * AB \\ & + 0.01175 * AC \\ & + 0.02325 * BC \\ & - 0.058375 * A^2 \\ & - 0.010375 * B^2 - 0.004375 * C^2 \end{aligned} \quad (6)$$

$$R2=3.98+0.27*A+0.98*B-0.22*C+0.14*AB-0.14*AC+0.37*BC-0.43\,A^2-0.51*B^2-0.10*C^2 \quad (7)$$

The significance of the fit of the second-order polynomial for the R1 and R2 was observed by carrying out analysis of variance (ANOVA), with results shown in Tables 3, 4, and 5.

The squared correlation coefficient (R^2) of the model was 0.9935 and 0.9899 for R1 and R2, respectively (Table 3), meaning that 99.35% (R1) and 98.99% (R2) of variation was explained by the model and only 0.65% and 1.01% of variation was a result of chance. This indicated that the model adequately represented the real relationship between the factors. The coefficient of variation (C.V.) obtained was 1.37% and 3.67% for R1 and R2, respectively. The low value of C.V. indicated a high reliability of the experiment[27, 28]. Adequate precision measured the signal to noise ratio, where ratio greater than 4 (R1, 34.868 and R2, 27.307) is desirable[29].

From results obtained in Table 4 for sphericity (R1), values of "Prob. > F" less than 0.05 indicated that the model terms were significant. Values greater than 0.10 indicated that the model terms were not significant. A model F-value of 118.59 and a very low probability value (Prob > F) less than 0.05 implied a significant model fit. From the regression model, the model terms A, B, and A^2 were significant model terms. The terms AB and BC were also significant model terms. This indicated that there was an interaction between extrusion temperature and feeding rate as well as between feeding rate and screw speed. However, the interaction between extrusion temperature and screw speed had no significant effect on pellet sphericity.

By increasing the extrusion temperature, the pellets that reached the cyclone were still soft and viscous during rotation, which helped them contract and become more spherical. Viscous forces like surface tension acted as a driving force and worked synergistically with the high rotation speed inside the cyclone. In contrast, lower extrusion temperature did not allow the pellets to reach the cyclone while they were in the soft and viscous form. The air that pushed them through the pipe can cause them not to be as soft as pellets extruded at higher temperature. The same principle applied to the feeding rate, as a high feeding rate brought more material to the cyclone. More material could retain heat and remained soft, whereas a small amount of material cooled quickly. Increasing the feeding rate improved the sphericity even at a lower extrusion temperature. Increasing the extrusion temperature along with feeding rate resulted in high spherical pellets. The interaction between screw speed and feeding rate significantly affected pellet sphericity. Increasing the screw speed resulted in high shear and energy input, which enhanced the temperature of the material inside the extruder. Therefore, by increasing the feeding rate along with screw speed, the high amount of material that reserved more heat gained more heat from the high shearing force, making the pellets softer when they reach the cyclone. The longer they are still soft inside the cyclone, the greater likelihood the pellets will contract and become more spherical.

Regarding hardness (R2) (Table 5), a value of "Prob. > F" less than 0.05 indicated the model term was significant, whereas a value greater than 0.10 indicated the model term was not significant. A model F-value of 76.60 and a very low probability value [(Prob > F) less than 0.05] implied a significant model fit. From the regression model, the model terms A, B, C, A^2 and B^2 were significant model terms. Another significant model term was BC, where the interaction between feeding rate and screw speed significantly influenced pellet hardness.

The increase in sphericity was accompanied by an increase in hardness. The shape and size of the pellets (diameter and thickness) revealed how a given hot melt processing parameter affected pellet hardness. When comparing non-spherical pellets to highly spherical pellets, the highly spherical pellets offered a smaller area to the sensing jaw of the hardness tester. Thus, increasing the load per unit area delayed fracture, which further resulted in increased hardness. Increasing the extrusion temperature lowered the melt viscosity, which made the material flow faster inside the extruder and promoted die swell phenomena at the die plate, leading to larger pellets[30, 31]. In addition, increasing the temperature produced softer extrudate, which was exposed to sudden cooling. The sudden cooling caused rapid contraction of polymer subunits, which increased the entanglement of chains and decreased porosity, resulting in greater resistance to fracture. Increasing the feeding rate increased the size of pellets significantly. Increasing the output from the die plate led to larger pellets, which provided more resistance for pellets to break. Extrusion temperature and feeding rate were found to significantly affect pellet hardness. The increase in shearing force resulted in the generation of more heat, thus decreasing the melt viscosity. Material with low melt viscosity flowed faster, which increased the amount of output and, hence, the size of pellets. The interaction between feeding rate and screw speed resulted in increased pellet hardness. Since the feeding rate highly affected pellet hardness, it works synergistically with the high shearing force in making larger size pellets, and was hence increase the pellets resistance to break.

Optimization of HME conditions

In order to optimize the influence of different processing parameters on the sphericity and hardness of produced pellets, we generated response surface plots using the regression model. The three-dimensional (3D) plots were obtained by keeping one factor constant at the center point and changing the others within the giving range. The resulting response surface plots revealed the influence of processing parameters on pellet sphericity and hardness.

Figs. 2 to 4 show the response surface and corresponding contour plots for the optimization of pellet sphericity. Fig. 2 shows the response surface and corresponding contour plots for pellets sphericity as a function of processing temperatures and feeding rate. An increase in the processing temperature with an accompanying increase in feeding rate resulted in an increase in pellets sphericity. Fig. 3 shows the response surface and corresponding contour plots for pellets sphericity as a function of processing temperatures and screw speed. An increase in the processing temperature with an accompanying increase in screw speed resulted in an increase in pellets sphericity. Fig. 4 shows the response surface and corresponding contour plots for pellet sphericity as a function of feeding rate and screw

speed. It clearly shows that the pellet sphericity was improved by increasing feeding rate and screw speed.

Figs. 5 to 7 show the response surface and corresponding contour plots for the optimization of pellets hardness. Fig. 5 shows the response surface and corresponding contour plots for pellet hardness as a function of processing temperature and feeding rate. An increase in the feeding rate with an accompanying increase in processing temperature resulted in an increase in pellet hardness. Fig. 6 shows the response surface and corresponding contour plots for pellet hardness as a function of extrusion temperature and screw speed. The interaction between extrusion temperature and screw speed had no significant effect on pellet hardness. Fig. 7 shows the response surface and corresponding contour plots for pellet hardness as a function of feeding rate and screw speed. An increase in the feeding rate with an accompanying increase in screw speed resulted in an increase in pellet hardness.

From the obtained results, Formulations F6, F7, and F15 had the maximum sphericity and hardness compared to other formulations, such as F4 (Fig. 8). Formulation F12 had maximum sphericity and hardness, but the average size of the F12 formulation was outside the acceptable pellet size range (0.5–2 mm)[32] (Table 6). To confirm the sphericity test finding, aspect ratio was measured for all optimized formulations. The aspect ratio of optimized pellets formulations were found to be within the acceptable range, which is from 1–1.2 (Table 6).

Drug content analysis

The drug content of the pellets was affected by the different processing parameters. The drug content of F12 formulation was 78.81 ± 4.58%. Hence, at a lower processing temperature (135) and higher feeding rate (7%), Soluplus® exhibited higher viscosity, and drug diffusion in the polymer became more limited. This resulted in relatively poor mixing inside the extruder. The drug content of F6, F7, and F15 formulations was 105.82 ± 1.0%, 98.93 ± 3.34%, and 98.61± 2.46%, respectively (Table 6).

Based on sphericity, hardness, average size, and drug content analysis, formulations F6, F7, and F15 were the optimized formulations and chosen for further studies.

Differential scanning calorimetry

The DSC thermograms showed that pure CBZ was characterized by a single, sharp melting endotherm peak at 193 °C (Fig. 9). The optimized extruded pellets showed no thermal peak for CBZ. This indicated that CBZ was solubilized and converted into the amorphous form in the polymer melt during the extrusion process.

Drug release study

CBZ is an antiepileptic drug with poor water solubility (17.7 mg/L at 25°C, log P value of 2.45)[33]. It is considered a Class II drug according to the Biopharmaceutical Classification System (BCS), which is characterized by low water solubility and high permeability. Thus, the dissolution of pure CBZ in 900 ml of water was very low, exhibiting less than 20% dissolution by the end of 120 min. Soluplus® is an amphiphilic polymer that forms micelles

in solution, and hence, can work as a solubilizing agent for poorly water-soluble drugs[34]. Soluplus® can successfully enhance the solubility of CBZ at 10% drug loading and lower[35]. Drug release from all of the optimized pellet formulations demonstrated greater dissolution than the pure drug. The drug release from the F6, F7, and F15 formulations was more than 80% within 90 minutes. (Fig. 10). The release rate from the F6 formulation was faster than the F7 and F15 formulations. The drug release profile of F6 was assessed by similarity factor (f2 value) in comparison to F7 and F15. If the similarity factor is between 50 and 100, it would suggest that two release profiles are similar. The f2 value for the release profile between F7 and F6 is 50, whereas the f2 value between F15 and F6 is 53. The dissolution profile is therefore considered as similar. The slight difference in release rate can be attributed to the size of the pellets, as F6 pellets were smaller in size than F7 and F15 and hence erosion as well as diffusion rate may be changed. All pellet release profiles exhibited delayed release behavior. The spherical pellets have a smaller surface area that comes in contact with dissolution medium than the non-spherical pellets. Therefore, spherical pellets take longer to release the drug.

Physical Characterization Data of the Optimized Pellets

Hardness friability index (HFI)—A friability testing apparatus was used to determine weight loss of the pellets (as a percentage). In friability testing, no significant weight loss was observed, and all tested pellets were found to be of superior hardness (Table 7). These findings confirmed the excellent mechanical properties of pellets prepared by the continuous HME process.

Flowability—Highly spherical pellets flow easily, which is considered ideal for further processing. From data presented in Table 7, the F6 pellet formulation flowed more easily than F7 and F17. This could be attributed to the fact that small size pellets flow more freely from the orifice than large size pellets.

Bulk density, tapped density and Carr's index—In the pharmaceutics field, Carr's index is used as another indicator of flowability. A Carr's index more than 25 indicates poor flow properties, and less than 15 indicates good flow properties[36, 37]. Highly spherical pellets occupy less volume, and there is not much difference between the value of bulk and tapped density. In Table 7, the values of bulk and tapped density for all optimized formulations were very close. The Carr's index of all optimized pellet formulations was less than 15.

CONCLUSION

The Box-Behnken experimental design was successfully utilized for the optimization of HME connected to a face-cut pelletizer, required only 17 experiments. Pellets with satisfactory physico-mechanical characteristics were successfully prepared by melt extrusion/face-cut pelletization using the optimized conditions. The present study discusses the development of novel, "ready to fill" face-cut pellets as final/finished drug products using HME techniques. These studies may be beneficial for optimizing the manufacture of

other types of dosage forms. Changing face cutter speed is a point of interest for future work.

References

1. Abrahamsson B, Alpsten M, Jonsson UE, Lundberg PJ, Sandberg A, Sundgren M, Svenheden A, Tölli J. Gastro-Intestinal Transit of a Multiple-Unit Formulation (Metoprolol Cr/Zok) and a Non-Disintegrating Tablet with the Emphasis on Colon. Int J Pharm. 1996; 140:229–235.
2. Crowley MM, Zhang F, Repka MA, Thumma S, Upadhye SB, Battu SK, McGinity JW, Martin C. Pharmaceutical Applications of Hot-Melt Extrusion: Part I. Drug Dev Ind Pharm. 2007; 33:909–926. [PubMed: 17891577]
3. Hulsmann S, Backensfeld T, Keitel S, Bodmeier R. Melt Extrusion–an Alternative Method for Enhancing the Dissolution Rate of 17beta-Estradiol Hemihydrate. Eur J Pharm Biopharm. 2000; 49:237–242. [PubMed: 10799815]
4. Leuner C, Dressman J. Improving Drug Solubility for Oral Delivery Using Solid Dispersions. Eur J Pharm Biopharm. 2000; 50:47–60. [PubMed: 10840192]
5. Tiwari RV, Patil H, Repka MA. Contribution of Hot-Melt Extrusion Technology to Advance Drug Delivery in the 21st Century. Expert Opin Drug Deliv. 2015:1–14.
6. Breitenbach J. Melt Extrusion: From Process to Drug Delivery Technology. Eur J Pharm Biopharm. 2002; 54:107–117. [PubMed: 12191680]
7. Repka MA, Battu SK, Upadhye SB, Thumma S, Crowley MM, Zhang F, Martin C, McGinity JW. Pharmaceutical Applications of Hot-Melt Extrusion: Part II. Drug Dev Ind Pharm. 2007; 33:1043–1057. [PubMed: 17963112]
8. Lang B, McGinity JW, Williams RO 3rd. Hot-Melt Extrusion- Basic Principles and Pharmaceutical Applications. Drug Dev Ind Pharm. 2014; 40(9):1133–1155. [PubMed: 24520867]
9. Daniel Treffer, SS. Pellet Production by Hot Melt Extrusion and Die Face Pelletising. 2013. http://www.pssrc.org/news/89. [Accessed Feb. 12, 2016]
10. Alshahrani SM, Morott JT, Alshetaili AS, Tiwari RV, Majumdar S, Repka MA. Influence of Degassing on Hot-Melt Extrusion Process. Eur J Pharm Sci. 2015; 80:43–52. [PubMed: 26296861]
11. A Ashour E, et al. Influence of Pressurized Carbon Dioxide on Ketoprofen-Incorporated Hot-Melt Extruded Low Molecular Weight Hydroxypropylcellulose. Drug Dev Ind Pharm. 2015:1–8. [PubMed: 25997363]
12. Alshetaili A, et al. Preparation and Evaluation of Hot-Melt Extruded Patient-Centric ketoprofen mini-Tablets. Curr Drug Deliv. 2015
13. Treffer D, et al. In-Line Implementation of an Image-Based Particle Size Measurement Tool to Monitor Hot-Melt Extruded Pellets. Int J Pharm. 2014; 466:181–189. [PubMed: 24614578]
14. Lustig-Gustafsson C, Kaur Johal H, Podczeck F, Newton JM. The Influence of Water Content and Drug Solubility on the Formulation of Pellets by Extrusion and Spheronisation. Eur J Pharm Sci. 1999; 8:147–152. [PubMed: 10210738]
15. Vervaet C, Baert L, Remon JP. Extrusion-Spheronisation a Literature Review. Int J Pharm. 1995; 116:131–146.
16. Young CR, Koleng JJ, McGinity JW. Production of Spherical Pellets by a Hot-Melt Extrusion and Spheronization Process. Int J Pharm. 2002; 242:87–92. [PubMed: 12176229]
17. Roblegg E, Jäger E, Hodzic A, Koscher G, Mohr S, Zimmer A, Khinast J. Development of Sustained-Release Lipophilic Calcium Stearate Pellets Via Hot Melt Extrusion. Eur J Pharm Biopharm. 2011; 79:635–645. [PubMed: 21801834]
18. Bialleck S, Rein H. Preparation of Starch-Based Pellets by Hot-Melt Extrusion. Eur J Pharm Biopharm. 2011; 79:440–448. [PubMed: 21570466]
19. Manivannan R, Parthiban KG, Sandeep G, Balasubramaniam A, Senthilkumar N. Multiparticlate Drug Delivery Systems: Pellet & Pelletization Technique. Drug invent today. 2010; 2:233–237.
20. Heng PW, Wong TW, Chan LW. Influence of Production Variables on the Sphericity of Melt Pellets. Chem Pharm Bull (Tokyo). 2000; 48:420–424. [PubMed: 10726869]

21. Jawahar N, Anilbhai PH. Multi Unit Particulates Systems (Mups): A Novel Pellets for Oral Dosage Forms. J Pharm Sci & Res. 2012; 4:1915–1923.
22. Alshahrani SM, et al. Stability-Enhanced Hot-Melt Extruded Amorphous Solid Dispersions Via Combinations of Soluplus(R) and Hpmcas-Hf. AAPS PharmSciTech. 2015; 16:824–834. [PubMed: 25567525]
23. Abbaspour MR, Sadeghi F, Garekani HA. Preparation and Characterization of Ibuprofen Pellets Based on Eudragit Rs Po and Rl Po or Their Combination. Int J Pharm. 2005; 303:88–94. [PubMed: 16153792]
24. Gowda D, Ravi V, Shivakumar H, Hatna S. Preparation, Evaluation and Bioavailability Studies of Indomethacin-Bees Wax Microspheres. J Mater Sci Mater Med. 2009; 20:1447–1456. [PubMed: 19277848]
25. Krogars K, Heinämäki J, Vesalahti J, Marvola M, Antikainen O, Yliruusi J. Extrusion–Spheronization of Ph-Sensitive Polymeric Matrix Pellets for Possible Colonic Drug Delivery. Int J Pharm. 2000; 199:187–194. [PubMed: 10802412]
26. Behera B, Sahoo S, Dhal S, Barik B, Gupta B. Characterization of Glipizide-Loaded Polymethacrylate Microspheres Prepared by an Emulsion Solvent Evaporation Method. Trop J Pharm Res. 2008; 7:879–885.
27. DC, M. Design and Analysis of Experiments. New York John Wiley & Sons Inc; 2008.
28. Mason, LR.; G, R. Statistical Design & Analysis of Experiments, Second Ed. New York: John Wiley & Sons Inc; 2003.
29. Kaur G, Rath G, Heer H, Goyal AK. Optimization of Protocell of Silica Nanoparticles Using 3(2) Factorial Designs. AAPS PharmSciTech. 2012; 13:167–173. [PubMed: 22173376]
30. Gavis J, Modan M. Expansion and Contraction of Jets of Newtonian Liquids in Air: Effect of Tube Length. Phys Fluids (1958–1988). 1967; 10:487–497.
31. Hiemenz, PC.; Lodge, TP. Polymer Chemistry. CRC press; 2007.
32. Schilling SU, Shah NH, Malick AW, McGinity JW. Properties of Melt Extruded Enteric Matrix Pellets. Eur J Pharm Biopharm. 2010; 74:352–361. [PubMed: 19782133]
33. Bertilsson L, Tomson T. Clinical Pharmacokinetics and Pharmacological Effects of Carbamazepine and Carbamazepine-10,11-Epoxide. An Update. Clin Pharmacokinet. 1986; 11:177–198. [PubMed: 3524954]
34. Hardung H, D D, Ali S. Combining Hme & Solubilization: Soluplus®—the Solid Solution. Drug Delivery Technology. 2010; 10:20–27.
35. Djuris J, Nikolakakis I, Ibric S, Djuric Z, Kachrimanis K. Preparation of Carbamazepine–Soluplus® Solid Dispersions by Hot-Melt Extrusion, and Prediction of Drug–Polymer Miscibility by Thermodynamic Model Fitting. Eur J Pharm Biopharm. 2013; 84:228–237. [PubMed: 23333900]
36. Bouffard J, Dumont H, Bertrand F, Legros R. Optimization and Scale-up of a Fluid Bed Tangential Spray Rotogranulation Process. Int J Pharm. 2007; 335:54–62. [PubMed: 17166677]
37. Shah RB, Tawakkul MA, Khan MA. Comparative Evaluation of Flow for Pharmaceutical Powders and Granules. AAPS PharmSciTech. 2008; 9:250–258. [PubMed: 18446489]

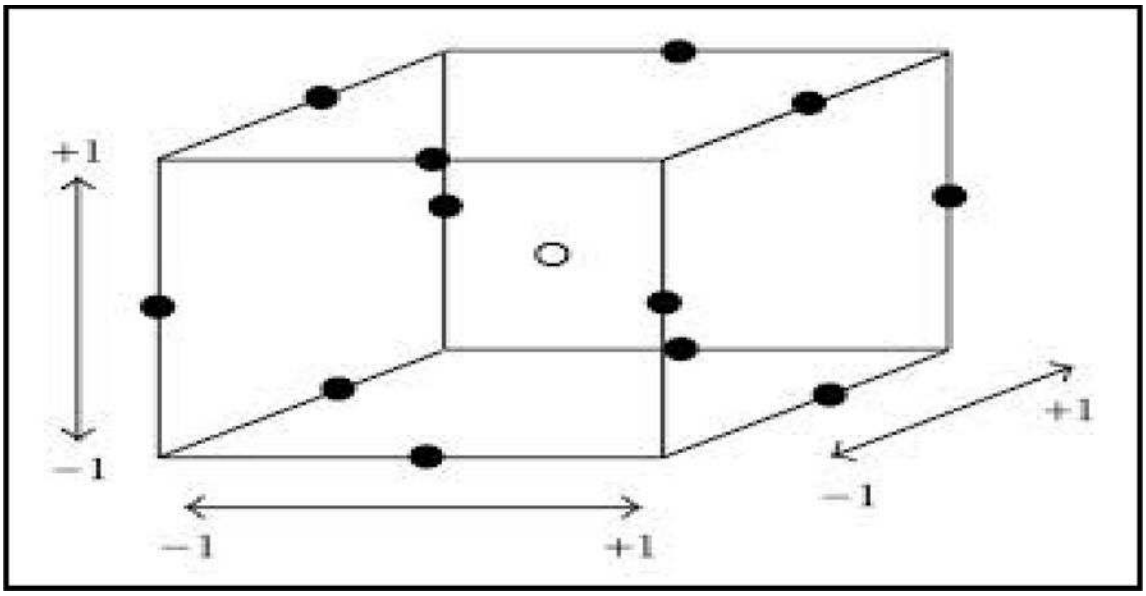

Fig. 1.
A three-dimensional representation in space of 3 Levels, 3 Factors Box-Behnken Design.

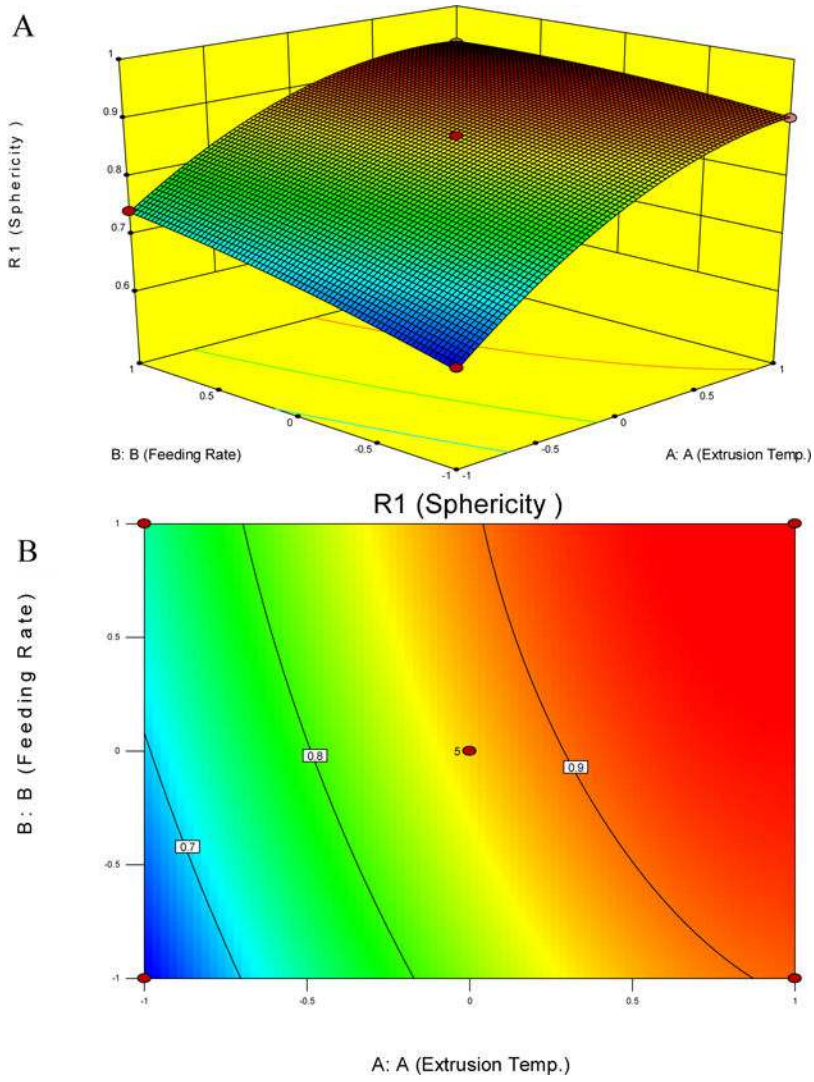

Fig. 2.

The response surface (A) and corresponding contour (B) plots for pellets' sphericity as a function of processing temperatures (°*C)* and feeding rate (%).

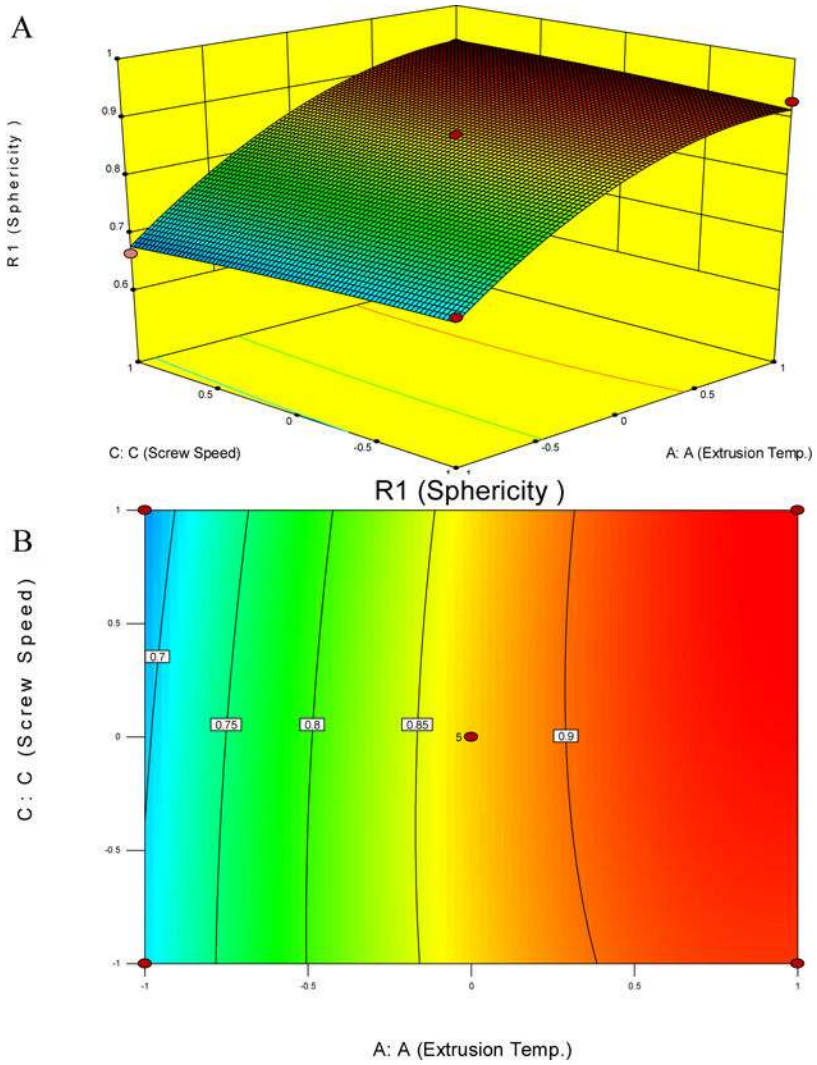

Fig. 3.

The response surface (A) and corresponding contour (B) plots for pellets' sphericity as a function of processing temperatures (°*C)* and screw speed (rpm).

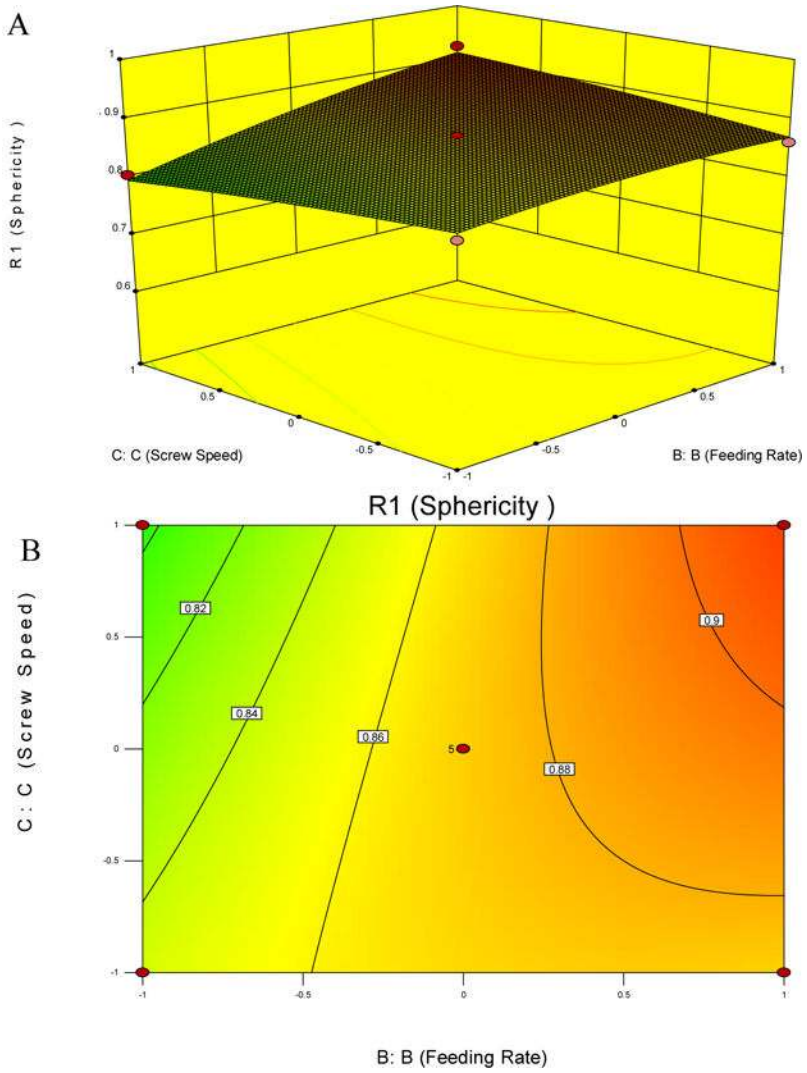

Fig. 4.

The response surface (A) and corresponding contour (B) plots for pellets' sphericity as a function of feeding rate (%) and screw speed (rpm).

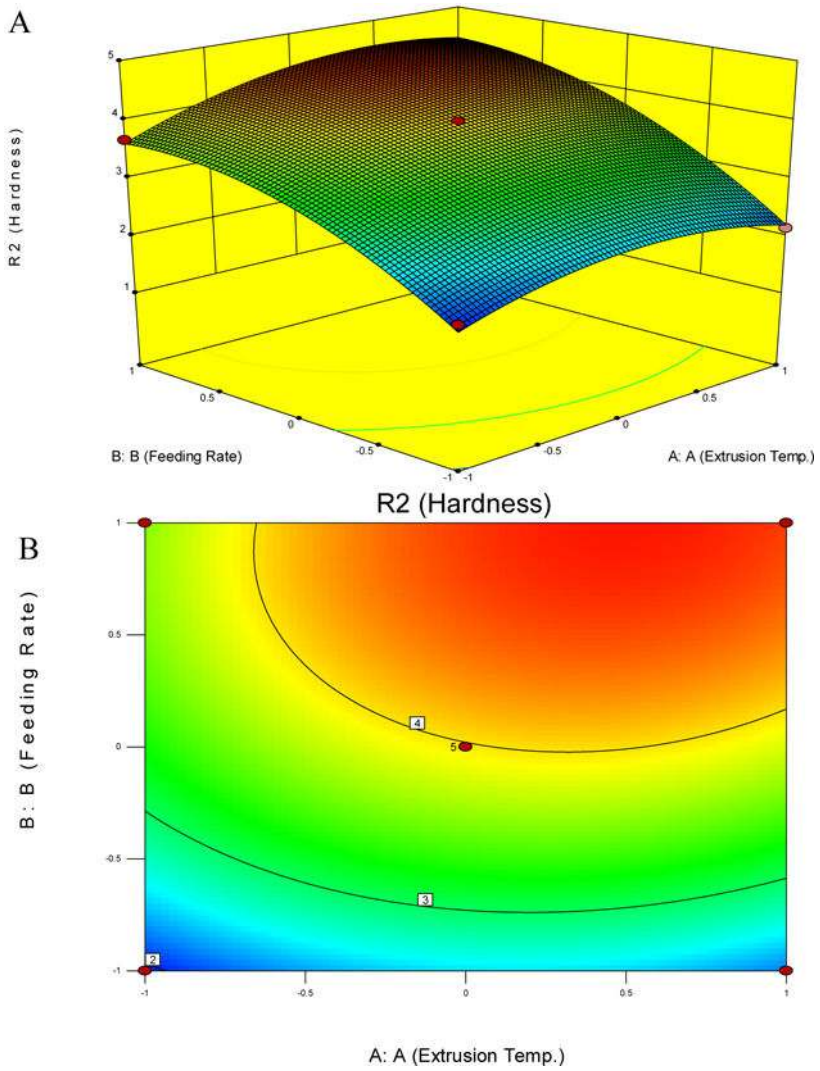

Fig. 5.

The response surface (A) and corresponding contour (B) plots for pellets' hardness as a function of processing temperatures (°*C)* and feeding rate (%).

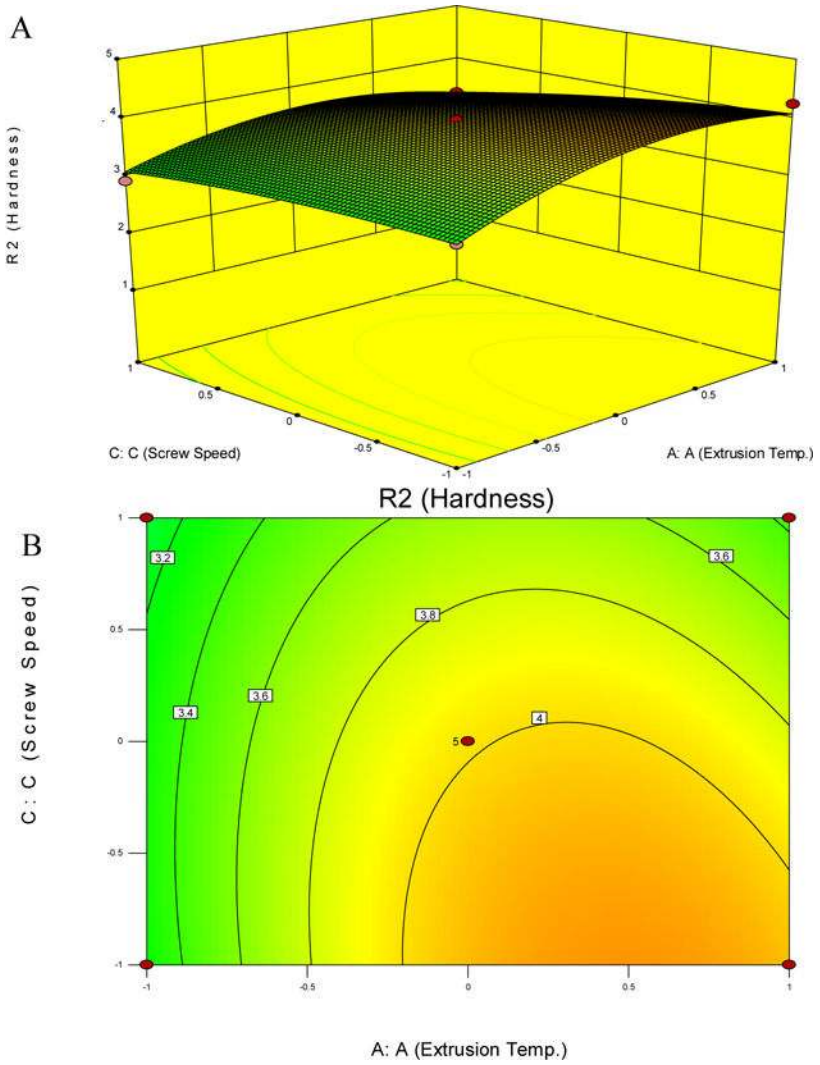

Fig. 6.

The response surface (A) and corresponding contour (B) plots for pellets' hardness as a function of processing temperatures (°*C)* and screw speed (rpm).

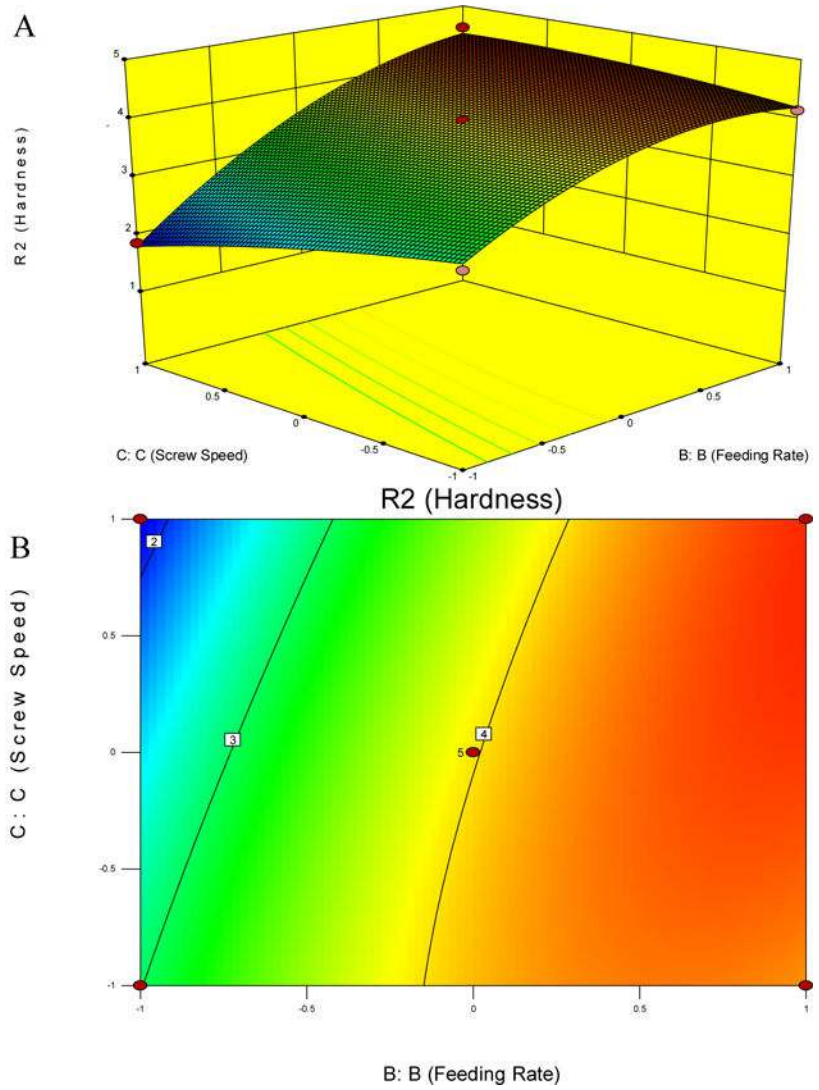

Fig. 7.

The response surface (A) and corresponding contour (B) plots for pellets' hardness as a function of feeding rate (%) screw speed (rpm).

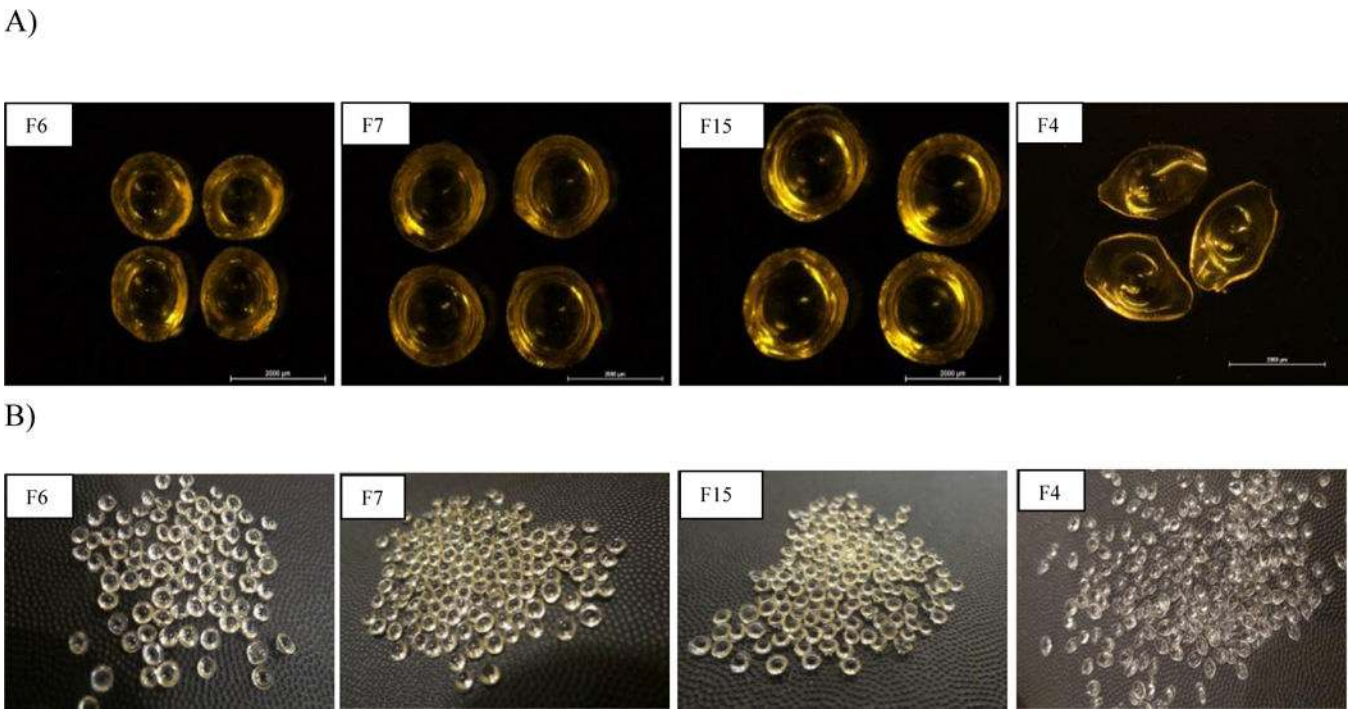

Fig. 8.
A) Microscopic and B) digital images of optimized formulations and negative control (F4).

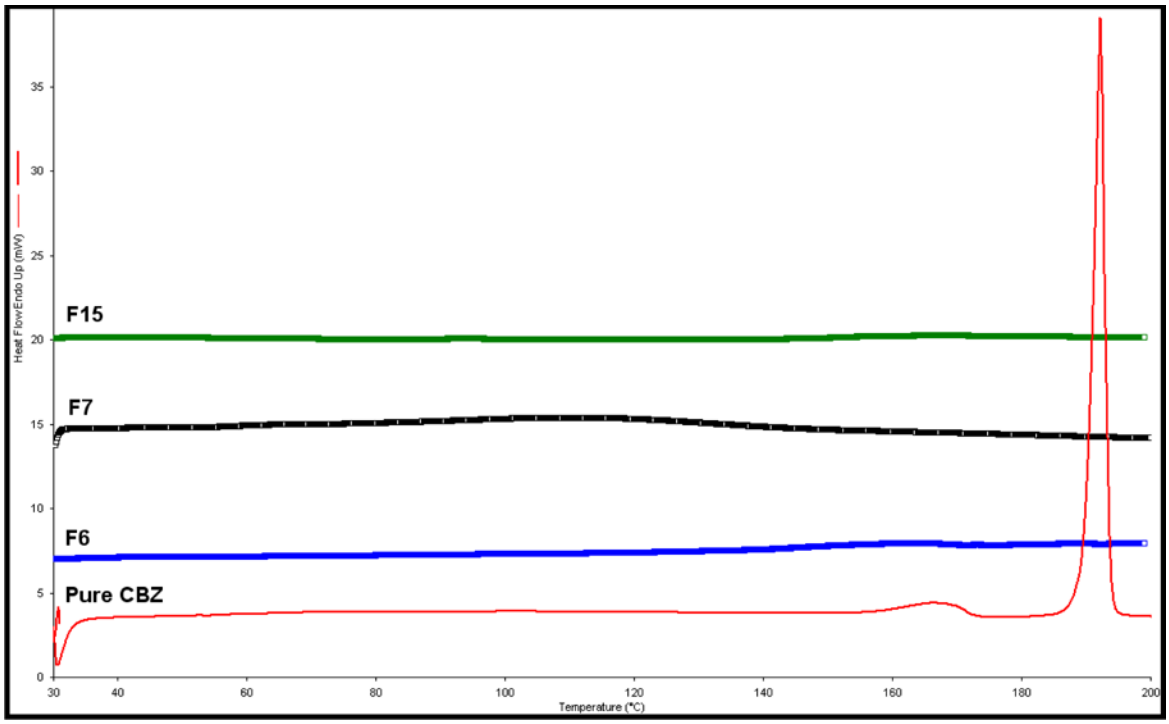

Fig. 9.
DSC thermogram of pure carbamazepine (CBZ) and extrudate utilizing Soluplus® matrices.

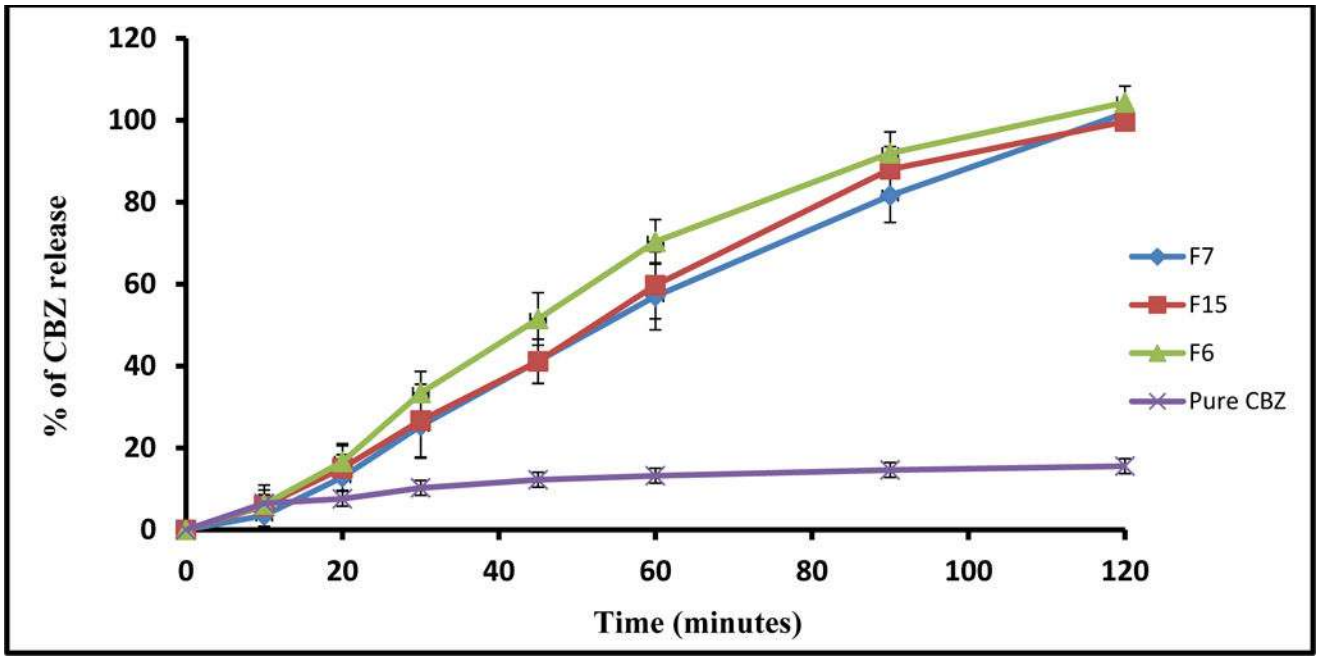

Fig. 10.
Carbamazepine dissolution profiles (Type II) in 900 ml of water at 100 rpm (n=3).

Table 1

The three factors of Box-Behnken design.

Variables	Symbol	Levels		
		−1	0	+1
Processing Temp (°C)	A:A	120	135	150
Feeding rate (%)	B:B	3	5	7
Screw speed (rpm)	C:C	100	150	200

Table 2

Three factors of Box-Behnken design with experimental as well as predicted responses of independent variable

Runs	A:A	B:B	C: C	Observed Sphericity R1	Predicted Sphericity R1	Observed Hardness R2 (kPa)	Predicted Hardness R2 (kPa)
F1	135	3	100	0.834	0.845	2.88	2.98
F2	135	7	100	0.861	0.870	4.15	4.20
F3	135	5	150	0.871	0.871	3.98	3.98
F4	120	3	150	0.634	0.630	2.05	1.94
F5	120	7	150	0.742	0.740	3.67	3.61
F6	150	5	200	0.928	0.936	3.37	3.36
F7	150	7	150	0.931	0.935	4.32	4.43
F8	135	5	150	0.871	0.871	3.98	3.98
F9	120	5	100	0.712	0.704	3.26	3.27
F10	120	5	200	0.665	0.678	2.93	3.09
F11	135	5	150	0.871	0.871	3.98	3.98
F12	135	7	200	0.925	0.913	4.60	4.49
F13	135	3	200	0.805	0.796	1.86	1.80
F14	150	3	150	0.902	0.903	2.15	2.21
F15	150	5	100	0.928	0.915	4.25	4.08
F16	135	5	150	0.871	0.871	3.98	3.98
F17	135	5	150	0.871	0.871	3.98	3.98

Table 3

Statistical information (ANOVA)

Source	R1 value	R2 value
R-squared	0.9935	0.9899
Adjusted R-squared	0.9851	0.9770
Standard deviation	0.011	0.13
C.V %	1.37	3.67
Adeq. precision	34.868	27.307

Table 4

Analysis of variance (ANOVA) for quadratic model of sphericity (R1)

Source	Sum of Squares	df	Mean Square	F Value	p-value [Prob > F]	
Model	0.14	9	0.015	118.59	< 0.0001	significant
A-A	0.11	1	0.11	839.17	< 0.0001	
B-B	0.010	1	0.010	77.26	< 0.0001	
C-C	1.800E-005	1	1.800E-005	0.14	0.7213	
AB	1.560E-003	1	1.560E-003	11.96	0.0106	
AC	5.522E-004	1	5.522E-004	4.23	0.0787	
BC	2.162E-003	1	2.162E-003	16.57	0.0047	
A^2	0.014	1	0.014	109.95	< 0.0001	
B^2	4.532E-004	1	4.532E-004	3.47	0.1047	
C^2	8.059E-005	1	8.059E-005	0.62	0.4577	
Residual	9.135E-004	7	1.305E-004			
Lack of Fit	9.135E-004	3	3.045E-004			
Pure Error	0.000	4	0.000			
Cor Total	0.14	16				

Table 5

Analysis of variance (ANOVA) for quadratic model of Hardness (R2)

Source	Sum of Squares	df	Mean Square	F Value	p-value [Prob > F]	
Model	11.33	9	1.26	76.60	< 0.0001	significant
A-A	0.59	1	0.59	36.14	0.0005	
B-B	7.60	1	7.60	462.71	< 0.0001	
C-C	0.40	1	0.40	24.10	0.0017	
AB	0.076	1	0.076	4.60	0.0691	
AC	0.076	1	0.076	4.60	0.0691	
BC	0.54	1	0.54	32.87	0.0007	
A^2	0.77	1	0.77	46.55	0.0002	
B^2	1.08	1	1.08	65.66	< 0.0001	
C^2	0.043	1	0.043	2.63	0.1491	
Residual	0.12	7	0.016			
Lack of Fit	0.12	3	0.038			
Pure Error	0.000	4	0.000			
Cor Total	11.45	16				

Table 6

The mean size and drug content of pellets with maximum sphericity and hardness

Formulations	Average Size (mm)	Aspect Ratio	Drug Content (%)
F6	1.62	1.026	105.82% ± 1.0
F7	2.06	1.028	98.93% ± 3.34
F15	1.85	1.037	98.61% ± 2.46

Table 7

Physical characterization data of the optimized pellets.

Formulation	Flowability ($gm.s^{-1}$)	HFI (%)	Bulk density (gm/cc)	Tapped density (gm/cc)	Carr's index (%)
F6	5.61	0.17	0.767	0.826	7.14
F7	5.35	0.16	0.773	0.830	7.37
F15	5.42	0.16	0.771	0.842	8.43